High Pressure Induced Formation of Carbon Nanorods from Tetracosane

Jiaxu Liang[‡, 1], *Christopher P. Ender*[‡, 1], *Pascal Rohrbeck*[1], *Robert Graf*[1], *Ingo Lieberwirth*[1], *Manfred Wagner*[1], *Stefan A. L. Weber*[1, 2], *Klaus Müllen*[1, 3] *and Tanja Weil*[*, 1]

1 Max Planck Institute for Polymer Research, Ackermannweg 10, 55128 Mainz, Germany

2 Institute of Physics, Johannes Gutenberg University Mainz, Duesbergweg 10-14, 55128 Mainz, Germany.

3 Department of Chemistry, University of Cologne, Greinstr. 4-6, 50939 Cologne, Germany

KEYWORDS: carbon nanorods, high-pressure high-temperature synthesis, morphology control

ABSTRACT: Morphology control of carbon nanostructures is essential for improving their performance in many applications. Direct pyrolysis of organic precursors, however, usually yields bulk amorphous carbon. Therefore, traditional methods for controlling the morphology of carbon nanostructures involve multistep processes and complex precursor molecules. While various methods have been developed under ambient pressure, the impact of pressure on the morphology of the resulting carbon nanostructures remains unexplored. Herein, we present the synthesis of carbon nanorods by direct pyrolysis of the low-cost aliphatic hydrocarbon tetracosane under high pressure conditions. The diameters of the carbon nanorods are adjusted by simply varying the

synthetic pressures. High pressure allows controlling both the nanorod morphology as well as the degree of order, and local conductivity of the thus prepared nanorods has been confirmed by conductive AFM measurements. Our method promises a convenient strategy to synthesize carbon nanostructures with controlled morphology and high ordered chemical structure, which opens opportunities for potential electronic and electrochemical applications.

INTRODUCTION

Carbon nanostructures have received much attention as functional elements in electrochemical devices, for gas adsorption and storage, as catalysts, and drug delivery systems based on their unique morphologies[1–3]. Specifically, one-dimensional (1D) nanostructures offer unique advantages due to their inherent high-aspect-ratio structural feature. 1D nanostructures can assemble into interconnected networks for flexible electronic materials with improved mechanical elasticity compared to bulk materials or sphere-like nanoparticles[4]. The 1D configuration can also provide continuous ion/electron channels and short diffusion distance for electrolyte ions when they are used in electrochemical devices[5, 6]. But convenient synthesis of well-defined 1D carbon nanostructures remains a major challenge because the pyrolysis process for the preparation of carbon materials normally gives amorphous structures. To obtain 1D carbon nanostructures, templates are widely used such as anodic aluminum oxide or mesoporous silica[3]. Alternatively, carbon nanorods have been synthesized by thermal transformation of rod-shaped metal–organic frameworks[7] or electrochemical deposition of a large polycyclic aromatic hydrocarbon (PAH)[8]. These methods, however, involve multistep wet chemistry processes, expensive precursors or hazardous chemicals, and the sizes of the products are difficult to adjust due to the limitation of

the templates or precursors. Noteworthy, these traditional methods are in most cases conducted under ambient pressure. However, pressure represents an important parameter that affects chemical bonds, phase transformation and thermodynamic properties of materials[9]. Exploring the synthesis of carbon nanostructures at higher pressures, particular in the gigapascal (GPa) range, could provide access to controlled nanoscale morphologies.

High-pressure studies of the interactions, reactions, and transformations of atoms or molecules have attracted emerging interest[10, 11]. In recent years, due to the availability of experimental high-pressure techniques, various atypical inorganic compounds such as $NaCl_3$[12], LaH_{10}[13], and Na_2He[14] have been synthesized at pressures up to 100–200 GPa and surprising material properties have been discovered. For example, elements that are insulators at ambient pressure become superconducting metals through structural phase transitions when the pressure is increased to over 100 GPa[15]. These experiments clearly demonstrate that chemical reactions often proceed in an unpredictable fashion and new materials with exciting properties can be formed under high pressure.

In the case of carbon materials, high pressure enables phase transition of carbon, along with the transformation from sp^2-hybridized to sp^3-hybridized atoms[16]. Therefore, high-pressure high-temperature (HPHT) techniques are commonly used to synthesize diamonds from all kinds of carbon allotropes[17–19]. However, most studies on carbon materials under high pressure focus on phase transition or atomic valence change, whereas the effect of pressure on morphology control of carbon nanostructures remains largely unexplored.

Herein, we demonstrate the convenient high-pressure synthesis of 1D carbon nanorods by direct pyrolysis of the low-cost aliphatic hydrocarbon tetracosane in a convenient one-pot process

(Figure 1a). To the best of our knowledge, we report the first pressure-induced synthesis of carbon nanostructures with controlled morphologies. We demonstrate that changing the external pressure from 2.6 GPa to 4.0 GPa affords nanorods with tunable diameters, which opens new avenues for synthesizing customized carbon nanomaterials without the need to prepare structurally complex precursor molecules, solvent or catalysts.

RESULT AND DISCUSSION

HPHT synthesis of carbon nanorods was carried out in an end-loaded piston cylinder capable of holding approximate 80 mg, which was pressed and exposed to pressures up to 4.2 GPa (Figure 1a and S1). Tetracosane was used as precursor molecule, which is a low-cost and structurally simple, commercial aliphatic hydrocarbon. After increasing the pressure to 2.6 GPa, tetracosane was heated with a heating rate of 55 °C/min and maintained for 18 h at 550 °C and 2.6 GPa. The reaction yielded in a black powder, which was termed CNR-2.6. The powder was used after washing with dichloromethane, and scanning electron microscopy (SEM) analysis of the product revealed the formation of rod-shaped carbon nanostructures with dimensions of around 260 nm wide and typically 1–3 µm in length (Figure 1b and S2). Transmission electron microscopy (TEM) image analysis further confirmed the formation of carbon nanorods with uniform diameters (Figure 1c). For comparison, tetracosane was pyrolyzed at 550 °C but at low pressure in a degassed ampoule, and the resulting products consisted of amorphous carbon chunks (denoted as ACC) without any specific shape (Figure 1d), indicating the crucial role of pressure in the formation of carbon nanorods.

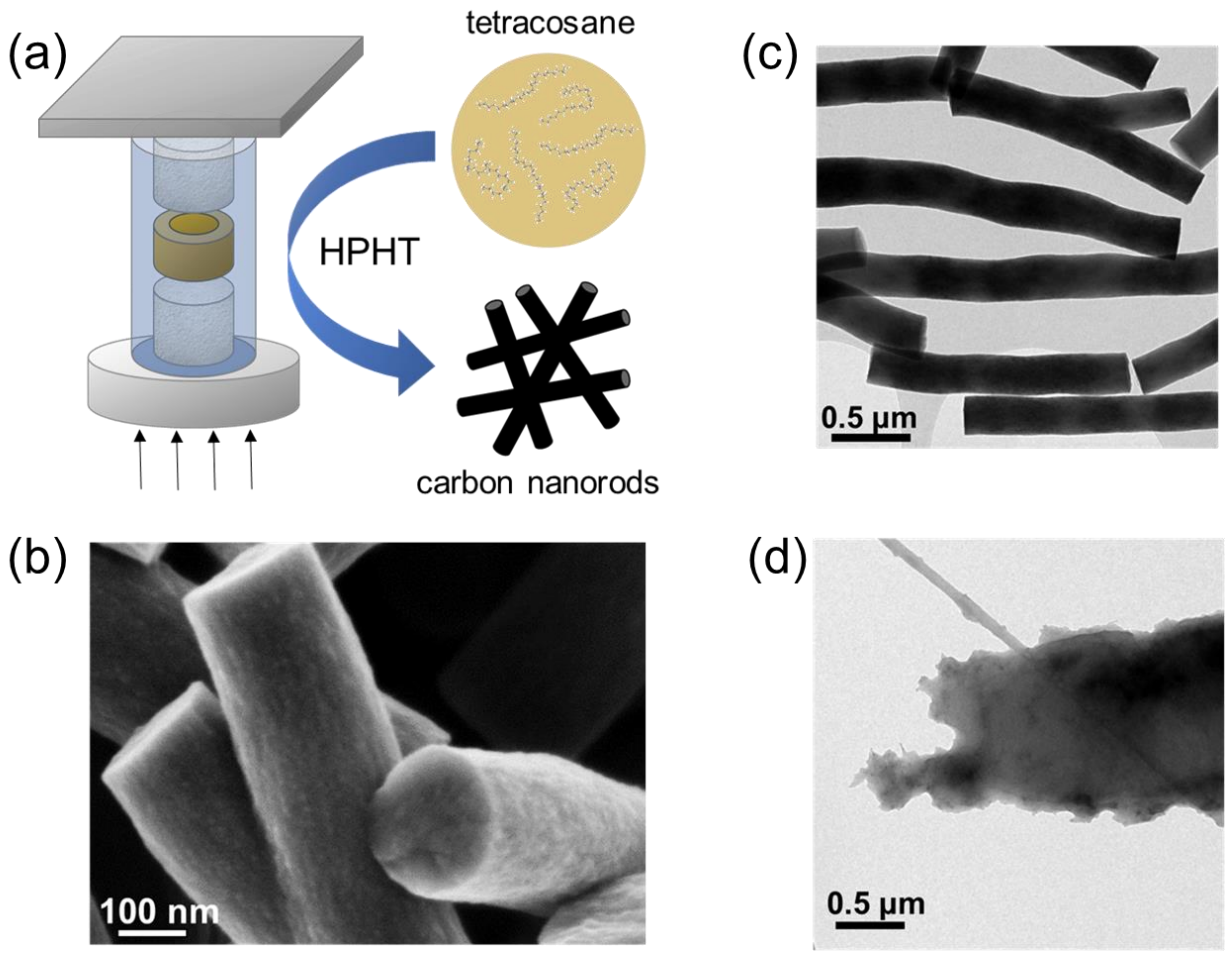

Figure 1. Synthesis of carbon nanorods from the aliphatic hydrocarbon tetracosane. (a) Illustration of HPHT synthesis of the carbon nanorods with a piston cylinder; (b) SEM image and (c) TEM image of the carbon nanorods synthesized at 550 °C and 2.6 GPa in a piston cylinder; (d) TEM image of the amorphous carbon chunk synthesized at low pressure in a degassed ampoule.

To elucidate the impact of pressure on the dimension of the thus formed carbon nanorods, HPHT experiments were conducted under different pressures. Specifically, the same precursor was heat-treated at 550 °C at 1.8 and 4.0 GPa. The recovered samples were denoted as CNR-1.8 and CNR-4.0, respectively. We found that the diameters of the carbon nanorods were remarkably affected by the synthesis pressures. The diameters of the recovered carbon nanorods could be adjusted as

652 ± 40 (CNR-1.8), 260 ± 25 (CNR-2.6), 106 ± 20 (CNR-4.0) nm (Figure 2 and Figure S3). That is, the diameters of the carbon nanorods reduced with the increase of the synthesis pressures. It was striking that the diameters could be adjusted in a broad range between 100 nm to 600 nm by applying around 2 GPa pressure. These results suggested that pressure could be an efficient tool to manipulate the morphology of carbon nanorods and this straight forward and clean approach could provide an alternative solution for the preparation of defined nanostructures also at larger scales.

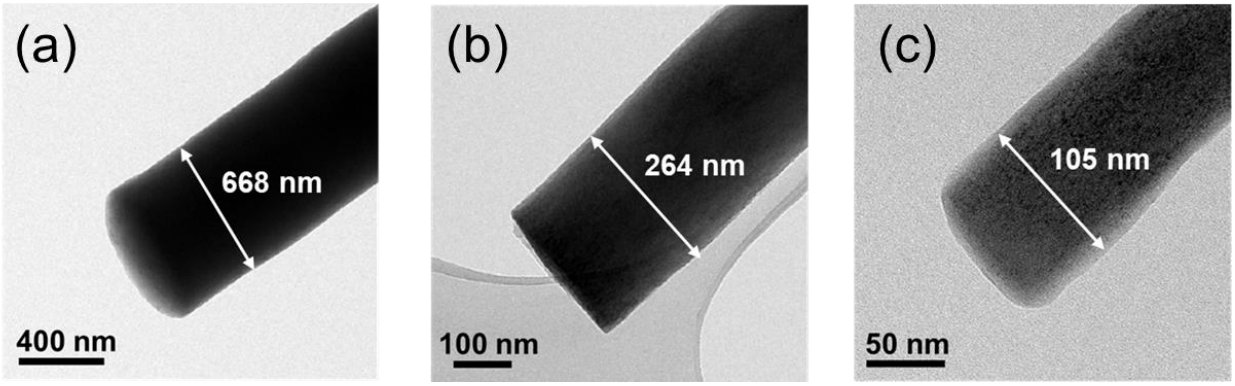

Figure 2. Carbon nanorods with various diameters synthesized under different pressures. (a) 1.8 GPa; (b) 2.6 GPa; (c) 4.0 GPa.

Besides morphology, intrinsic chemical structures represent also essential factors to improve the performance of carbon nanostructures in many applications. For example, dangling bonds and defective sites in carbon materials could contribute to their electrochemical reactivity and affect their conductivity when they are used as electrode materials[20, 21]. To investigate the impact of pressure on the chemical structures of the formed carbon nanorods, we characterized CNR-2.6 prepared under high pressure and compared it with ACC from low pressure synthesis. Energy dispersive X-ray spectroscopy (EDX) in Figure S4 revealed that carbon was the predominant

element in CNR-2.6 with trace amount of oxygen, which could be due to atmospheric oxygen adsorbed on the surface of the nanorod. The chemical structure of CNR-2.6 was further investigated by solid state nuclear magnetic resonance (NMR) with ^{1}H–^{13}C cross polarization (CP) magic angle spinning (MAS) measurement (Figure 3a). The intense peak at around 122 ppm represented aromatic carbons[22], while the broad asymmetric signal around 22 ppm is assigned to sp^3 carbon moieties. The ratio of sp^2 carbon to sp^3 carbon was estimated to be 95:5. Considering the broad and featureless ^{1}H signal, one could assume the presence of residual methyl groups and methylene in the carbon matrix, originating from the aliphatic precursor. Although a quantitative version[23] of the CP-MAS method has been applied, it should be noted that there might be a systematic tendency to overestimate the content of protonated sp^3 carbon. Powder X-ray diffraction (PXRD) revealed the crystalline structures of CNR-2.6 and ACC (Figure 3b). The characteristic peaks of the graphitic carbon (002) diffraction suggested that both samples were composed of graphitic carbon sheets. However, ACC exhibited a broad peak at 25.0°, whereas CNR-2.6 showed a much sharper peak, indicating larger domain sizes of the graphitic sheets after high-pressure synthesis[24]. Notably, the (002) peak position of CNR-2.6 was centered at 26.0°, larger than that of ACC and similar to that of graphite[24] suggesting that the distances between the graphitic sheets for CNR-2.6 were smaller indicating that high pressure resulted in more closely packed graphitic sheets. CNR-1.8 and CNR-4.0 also revealed similar XRD patterns with sharp peaks at around 26.0° (Figure S5). The crystalline lattices of CNR-2.6 were also visible under high-resolution TEM (Figure S6) and here, the graphitic sheets were oriented perpendicular to the rod axis. A dominant crystal plane corresponding to d-spacing of 3.6 Å was found by selected-area electron diffraction (SAED), which was close to the interplanar spacing of graphite and confirmed an ordered layer structure[25]. Raman I_D/I_G ratio (where I_D and I_G are D-band and G-

band Raman intensities) is another indicator widely used to evaluate the quality of carbon chemical structures[26]. The lower intensity ratio (I_D/I_G) of 0.81 for CNR-2.6 (Figure 3c), compared to 0.99 for ACC, implied the formation of higher ordered carbon structures under high-pressure synthesis[27], which was in accordance with the XRD and TEM results. The I_D/I_G of CNR-1.8 and CNR-4.0 were 0.84 and 0.81, respectively (Figure S7), which were similar to that of CNR-2.6. Our results clearly demonstrate that high pressure facilitated the formation of rod-shaped carbon nanostructures with increasing degree of order of the graphitic carbon sheets, leading to higher crystallinity and greater extend of graphitization.

The proposed mechanism of carbon nanorods formation under pressure is depicted in Figure 3d. First, tetracosane could decompose into PAHs[28, 29]; then these PAHs aggregated to form nucleation clusters of graphitic sheets and grew into the observed rod-shaped nanostructures. Usually, organic precursors form spherical nanoparticles under ambient pressure carbonization which aggregate into commonly observed carbon aerogels. Carbon nanostructures such as nanorods are rarely found because vectorial alignment towards nanorods requires anisotropic Hamaker interaction (force fields) between the graphitic particles[30]. This type of anisotropy could result from preferred orientation of graphitic sheets within the particles. In our case, high pressure could produce larger sized PAHs as suggested by the above structural characterization, which facilitated the cylindrical orientation of the graphitic sheets. Furthermore, high pressure could also directly provide an anisotropic force fields, thereby supporting the formation of carbon nanorods.

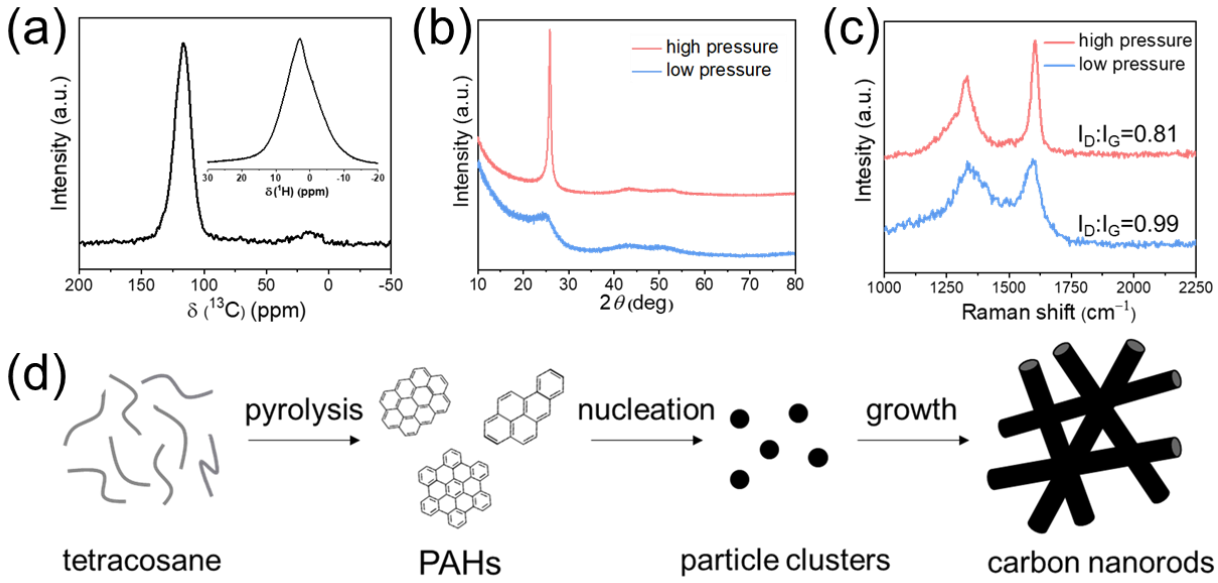

Figure 3. Structural characterization of the carbon nanorods. (a) Solid state NMR spectra of CNR-2.6 from 550 °C and 2.6 GPa; (b) XRD patterns and (c) Raman spectra of CNR-2.6 (red curves) and ACC (blue curves). (d) Proposed formation mechanism of the carbon nanorods.

The high degree of sp^2 hybridization suggested that the carbon nanorods were electrically conductive. To test the electrical properties, we performed conductive AFM (c-AFM) measurements, where the current between a nanoscale tip and the substrate was measured. Diluted suspensions of CNR-2.6 and CNR-1.8 nanoparticles were deposited on a Si-wafer coated with a thin platinum layer. During imaging, we had to take great care to avoid the sticking of nanorods to the AFM tip (Figure S8). We therefore selected the fast force mapping (FFM) mode, where a fast (10–100Hz) sequence of force-distance curves was performed up to a maximum predetermined load force (2.3 nN in our measurements) and simultaneously recorded the tip-sample current. The height of the individual carbon nanorod of CNR-2.6 was 227 ± 2 nm as shown in Figure 4(a), which was comparable to the TEM measurements. The current maps clearly showed that the carbon nanorods were electrically conductive with an average vertical current of 680 ± 20 pA

measured at a voltage of 10 mV. On the areas surrounding the nanorods, the direct contact between the metallic tip and the Pt substrate led to a saturation of the current amplifier. We also found a similar result on the CNR-1.8 nanorods (Figure S9). The conductivity value was comparable to carbon black despite that the synthetic temperature of these carbon nanorods was much lower. Furthermore, the 1D structure of nanorods has the advantage to construct conductive percolation network with small amount of material usage[4]. The local conductivity at the nanoscale would also promise electric inks for organic electronics.

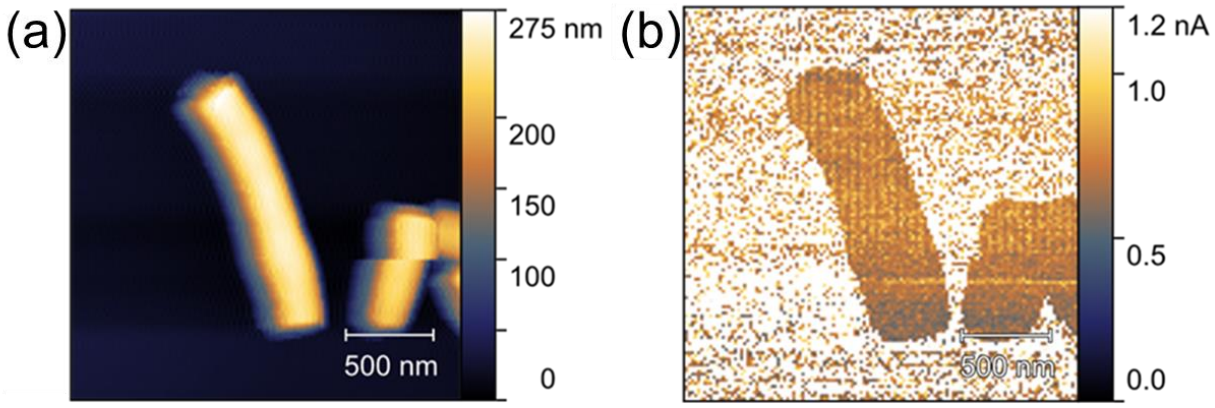

Figure 4. c-AFM result of CNR-2.6 captured in FFM mode. (a) Topography image of CNR-2.6. The asymmetry in the structure comes from the tip shape (tip convolution effect) (b) Maximum current of each pixel measured at a tip-sample voltage of 10 mV in FFM mode of CNR-2.6. The current signal went into saturation directly on the Pt electrode in the areas around the nanorods.

CONCLUSION

In summary, we report a convenient approach to synthesize carbon nanorods based on high pressure chemistry. Since traditional methods for carbon nanostructures are mostly conducted under ambient pressure, we extended the synthesis conditions to higher pressures, for the first time, to investigate the impact of pressure on the morphology control of the resultant carbon

nanostructures. Compared to the traditional methods that typically involve multistep reactions and hazardous chemicals, our method used the low-cost aliphatic hydrocarbon tetracosane as precursor in a solvent-free one-pot process. Moreover, the diameters of the carbon nanorods could be adjusted simply by controlling the synthesis pressures. Our results revealed that pressure, as a critical thermodynamic parameter, not only induced the formation of carbon nanorods but also had great impact on the chemical structure of carbon at an atomic level. The local conductivity at the nanoscale was confirmed by conductive AFM, which opens promising applications of these nanorods in electronic and electrochemical devices. We envision that high pressure could be potentially applied for the synthesis of other material systems where morphology control or high-quality crystals are crucial, such as semiconductor nanocrystals, nanostructured metal oxide and various 2D materials for catalysis, optics and magnetic applications.

ASSOCIATED CONTENT

Supporting Information.

The following files are available free of charge.

Materials, Methods and supplementary figures for the experiment setup and product characterizations (PDF)

AUTHOR INFORMATION

Corresponding Author

* Tanja Weil E-mail: weil@mpip-mainz.mpg.de

Author Contributions

The manuscript was written through contributions of all authors. All authors have given approval to the final version of the manuscript. ‡These authors contributed equally.

Notes

The authors declare no competing financial interest.

ACKNOWLEDGMENT

The authors are grateful for the financial support from the European Union's Horizon 2020 Research and Innovation Program under FETOPEN grant agreement no. 858149 (AlternativeToGd). The authors thank Gunnar Glaser for SEM measurements, Katrin Kirchhoff for EDX measurements, and Jan Weinheimer for machining the piston cylinder assemblies.

REFERENCES

(1) Wu, M.; Liao, J.; Yu, L.; Lv, R.; Li, P.; Sun, W.; Tan, R.; Duan, X.; Zhang, L.; Li, F.; Kim, J.; Shin, K. H.; Seok Park, H.; Zhang, W.; Guo, Z.; Wang, H.; Tang, Y.; Gorgolis, G.; Galiotis, C.; Ma, J. 2020 Roadmap on Carbon Materials for Energy Storage and Conversion. *Chem. Asian. J.* **2020**, *15* (7), 995–1013.

(2) Benzigar, M. R.; Talapaneni, S. N.; Joseph, S.; Ramadass, K.; Singh, G.; Scaranto, J.; Ravon, U.; Al-Bahily, K.; Vinu, A. Recent advances in functionalized micro and mesoporous carbon materials: synthesis and applications. *Chem. Soc. Rev.* **2018**, *47* (8), 2680–2721.

(3) Lu, A.-H.; Hao, G.-P.; Sun, Q.; Zhang, X.-Q.; Li, W.-C. Chemical Synthesis of Carbon Materials With Intriguing Nanostructure and Morphology. *Macromol. Chem. Phys.* **2012**, *213* (10-11), 1107–1131.

(4) Gong, S.; Cheng, W. One-Dimensional Nanomaterials for Soft Electronics. *Adv. Electron. Mater.* **2016**, *3* (3), 1600314.

(5) Wei, Q.; Xiong, F.; Tan, S.; Huang, L.; Lan, E. H.; Dunn, B.; Mai, L. Porous One-Dimensional Nanomaterials: Design, Fabrication and Applications in Electrochemical Energy Storage. *Adv. Mater.* **2017**, *29* (20), 1602300.

(6) Sun, H.; Deng, J.; Qiu, L.; Fang, X.; Peng, H., Recent progress in solar cells based on one-dimensional nanomaterials. *Energy Environ. Sci.* **2015**, *8* (4), 1139–1159.

(7) Pachfule, P.; Shinde, D.; Majumder, M.; Xu, Q., Fabrication of carbon nanorods and graphene nanoribbons from a metal-organic framework. *Nat. Chem.* **2016**, *8* (7), 718–724.

(8) Zeng, C.; Zheng, W.; Xu, H.; Osella, S.; Ma, W.; Wang, H. I.; Qiu, Z.; Otake, K. I.; Ren, W.; Cheng, H.; Müllen, K.; Bonn, M.; Gu, C.; Ma, Y., Electrochemical Deposition of a Single-Crystalline Nanorod Polycyclic Aromatic Hydrocarbon Film with Efficient Charge and Exciton Transport. *Angew. Chem. Int. Ed.* **2022**, *61* (13), e202115389.

(9) McMillan, P. F. Chemistry at high pressure. *Chem. Soc. Rev.* **2006**, *35* (10), 855–857.

(10) Miao, M.; Sun, Y.; Zurek, E.; Lin, H. Chemistry under high pressure. *Nat. Rev. Chem.* **2020**, *4* (10), 508–527.

(11) Zhang, L.; Wang, Y.; Lv, J.; Ma, Y. Materials discovery at high pressures. *Nat. Rev. Mater.* **2017**, *2* (4), 17005.

(12) Zhang, W.; Oganov, A. R.; Goncharov, A. F.; Zhu, Q.; Boulfelfel, S. E.; Lyakhov, A. O.; Stavrou, E.; Somayazulu, M.; Prakapenka, V. B.; Konôpková, Z. Unexpected Stable Stoichiometries of Sodium Chlorides. *Science* **2013**, *342* (6165), 1502–1505.

(13) Drozdov, A. P.; Kong, P. P.; Minkov, V. S.; Besedin, S. P.; Kuzovnikov, M. A.; Mozaffari, S.; Balicas, L.; Balakirev, F. F.; Graf, D. E.; Prakapenka, V. B.; Greenberg, E.; Knyazev, D. A.; Tkacz, M.; Eremets, M. I. Superconductivity at 250 K in lanthanum hydride under high pressures. *Nature* **2019**, *569* (7757), 528–531.

(14) Dong, X.; Oganov, A. R.; Goncharov, A. F.; Stavrou, E.; Lobanov, S.; Saleh, G.; Qian, G. R.; Zhu, Q.; Gatti, C.; Deringer, V. L.; Dronskowski, R.; Zhou, X. F.; Prakapenka, V. B.; Konopkova, Z.; Popov, I. A.; Boldyrev, A. I.; Wang, H. T. A stable compound of helium and sodium at high pressure. *Nat. Chem.* **2017**, *9* (5), 440–445.

(15) Buzea, C.; Robbie, K. Assembling the puzzle of superconducting elements: a review. *Supercond. Sci. Technol.* **2005**, *18* (1), R1–R8.

(16) Xie, Y. P.; Zhang, X. J.; Liu, Z. P. Graphite to Diamond: Origin for Kinetics Selectivity. *J. Am. Chem. Soc.* **2017**, *139* (7), 2545–2548.

(17) Dong, J.; Yao, Z.; Yao, M.; Li, R.; Hu, K.; Zhu, L.; Wang, Y.; Sun, H.; Sundqvist, B.; Yang, K.; Liu, B. Decompression-Induced Diamond Formation from Graphite Sheared under Pressure. *Phys. Rev. Lett.* **2020**, *124* (6), 065701.

(18) Crane, M. J.; Petrone, A.; Beck, R. A.; Lim, M. B.; Zhou, X.; Li, X.; Stroud, R. M.; Pauzauskie, P. J. High-pressure, high-temperature molecular doping of nanodiamond. *Sci. Adv.* **2019**, *5* (5), eaau6073.

(19) Pei, C.; Wang, L. Recent progress on high-pressure and high-temperature studies of fullerenes and related materials. *Matter Radiat. Extremes* **2019**, *4* (2), 028201.

(20) Tang, C.; Wang, H. F.; Chen, X.; Li, B. Q.; Hou, T. Z.; Zhang, B.; Zhang, Q.; Titirici, M. M.; Wei, F. Topological Defects in Metal-Free Nanocarbon for Oxygen Electrocatalysis. *Adv. Mater.* **2016**, *28* (32), 6845–6851.

(21) Zhu, J.; Huang, Y.; Mei, W.; Zhao, C.; Zhang, C.; Zhang, J.; Amiinu, I. S.; Mu, S. Effects of Intrinsic Pentagon Defects on Electrochemical Reactivity of Carbon Nanomaterials. *Angew. Chem. Int. Ed.* **2019**, *58* (12), 3859–3864.

(22) Wang, Z.; Opembe, N.; Kobayashi, T.; Nelson, N. C.; Slowing, I. I.; Pruski, M., Quantitative atomic-scale structure characterization of ordered mesoporous carbon materials by solid state NMR. *Carbon* **2018**, *131*, 102–110.

(23) Johnson, R. L.; Schmidt-Rohr, K. Quantitative solid-state ^{13}C NMR with signal enhancement by multiple cross polarization. *J. Magn. Reson.* **2014**, *239*, 44–49.

(24) Kim, T.-H.; Jeon, E. K.; Ko, Y.; Jang, B. Y.; Kim, B.-S.; Song, H.-K. Enlarging the d-spacing of graphite and polarizing its surface charge for driving lithium ions fast. *J. Mater. Chem. A* **2014**, *2* (20), 7600–7605.

(25) Mori, T.; Tanaka, H.; Dalui, A.; Mitoma, N.; Suzuki, K.; Matsumoto, M.; Aggarwal, N.; Patnaik, A.; Acharya, S.; Shrestha, L. K.; Sakamoto, H.; Itami, K.; Ariga, K. Carbon Nanosheets by Morphology-Retained Carbonization of Two-Dimensional Assembled Anisotropic Carbon Nanorings. *Angew. Chem. Int. Ed.* **2018**, *57* (31), 9679–9683.

(26) Jorio, A.; Souza Filho, A. G. Raman Studies of Carbon Nanostructures. *Annu. Rev. Mater. Res.* **2016**, *46* (1), 357–382.

(27) Zhou, J.; Lian, J.; Hou, L.; Zhang, J.; Gou, H.; Xia, M.; Zhao, Y.; Strobel, T. A.; Tao, L.; Gao, F. Ultrahigh volumetric capacitance and cyclic stability of fluorine and nitrogen co-doped carbon microspheres. *Nat. Commun.* **2015**, *6*, 8503.

(28) Ding, J.; Zhang, L.; Zhang, Y.; Han, K. L. A reactive molecular dynamics study of n-heptane pyrolysis at high temperature. *J. Phys. Chem. A* **2013**, *117* (16), 3266–3278.

(29) Martin, J. W.; Pascazio, L.; Menon, A.; Akroyd, J.; Kaiser, K.; Schulz, F.; Commodo, M.; D'Anna, A.; Gross, L.; Kraft, M. pi-Diradical Aromatic Soot Precursors in Flames. *J. Am. Chem. Soc.* **2021**, *143* (31), 12212–12219.

(30) Chang, Y.; Antonietti, M.; Fellinger, T. P. Synthesis of nanostructured carbon through ionothermal carbonization of common organic solvents and solutions. *Angew. Chem. Int. Ed.* **2015**, *54* (18), 5507–5512.

For Table of Contents Only